

Scientific paper

The Nanostructure Studies of Surfactant-Free-Microemulsions in Fragrance Tinctures

Perica Bošković,^{1*} Vesna Sokol,¹ Didier Touraud,² Ante Prkić³
and Josipa Giljanović³

¹ Department of Physical Chemistry, Faculty of Chemistry and Technology, University of Split, Teslina 10, 21000, Split, Croatia

² Institute of Physical and Theoretical Chemistry, University of Regensburg, D-93040 Regensburg, Germany

³ Department of Analytical Chemistry, Faculty of Chemistry and Technology, University of Split, Teslina 10, 21000, Split, Croatia

* Corresponding author: perica@ktf-split.hr

Phone: ++38521329444

Received: 08-10-2015

Abstract

As it was shown recently that nanostructures can exist in water-ethanol-citronellol tinctures, a deeper investigation of these media was performed using conductivity, UV-Vis and FT-IR spectroscopy techniques. Different regimes of conductivity, depending on the water content, an increase of the polarity of the polar pseudo-phase with increasing water content, and even the presence of free water molecules at higher water content are observed, just as in classical surfactant-based microemulsions. The percolation model, generally used to fit conductivity data in surfactant based microemulsion having a weak interfacial film, can be used to fit our conductivity data below a critical water content (ϕ_w^p) with a critical exponent typical of dynamic percolation. In presence of higher water contents, superior to ϕ_w^p , obtained conductivity data cannot be fitted neither with a static nor a dynamic percolation model. As in surfactant-based microemulsions, an increase of polarity of the microenvironment with increasing water content can be postulated using respectively the UV-Vis wavelength absorption band (λ_{\max}) of methyl orange and performing FT-IR spectra.

Keywords: Nanostructure, Citronellol, Microemulsions, UV-Vis spectroscopy, Conductivity, FT-IR spectroscopy

1. Introduction

Tinctures are alcoholic, mostly ethanol, solutions prepared from vegetable materials or from chemical substances as fragrance molecules. Tinctures are widely used as a base of hydro-alcoholic formulation produced in perfume industry. The terpenoids are the largest group of natural odorants, and thus also the largest group of modern fragrance ingredients.¹ Citronellol is one of the most important terpenoids, characteristic for the perfume industry. The main factors, which affect the volume of use of a fragrance ingredient, are its odour contribution to a fragrance, its stability and performance in the products to be perfumed. Recently we showed two interesting consequences in monophasic 1-octanol-ethanol-water mixtures for prac-

tical applications: the transition from “unstructured” to “structured” region along with a change of slope of conductivity that exists at high ethanol content, in a domain typically used for perfumes. Moreover, changes of slopes are also found when evaporation rates are plotted versus the amount of oil phase during the transition from o/w to w/o domains, a phenomenon that is widely used in formulation of long-lasting perfume formulation.²

According available literature only few recent studies reported the theoretical analysis based on the percolation phenomenon, which occurs as the microstructure of microemulsions changes.^{3–6}

Recently, the static and dynamic percolation models have been proposed for describing the mechanism of percolation.^{7,8} The static percolation theory describes the percolation to the appearance of a bicontinuous oil and water

structure, while the dynamic percolation model describes the formation of percolation clusters by interaction between water globules. The transport of ions in bicontinuous structure or percolation clusters gives rise to the percolation phenomenon.

Both models consider that the percolation transition takes place at a critical water mass fraction ϕ_w^p (percolation threshold). The power-laws between the conductivity and the concentration of hydrophilic (water) phase, below and above ϕ_w^p , are the following, respectively:

$$\begin{aligned} \kappa &\propto |\phi_w^p - \phi_w^{\square}|^{-s} \text{ for } \phi_w^p > \phi_w^{\square}, \\ \kappa &\propto |\phi_w^{\square} - \phi_w^p|^p \text{ for } \phi_w^p < \phi_w^{\square}, \end{aligned} \quad (1)$$

where s and p are critical exponents, $p \approx 1.5\text{--}2.0$ both in static and dynamic theory, $s \approx 0.5\text{--}0.7$ in static theory, $s \approx 1.0$ in dynamic theory.^{7,8}

In this article, the structure transition based on percolation mechanism of the Surfactant-Free-Microemulsion composed of citronellol, ethanol, and water was investigated using electrical conductivity, UV-Vis spectroscopy and FTIR spectra measurement.

2. Experimental

2.1. Chemicals

All chemicals used were of suitable laboratory reagent grade. Ethanol and citronellol were purchased from Merck Schuchardt OHG (Hohenbrunn, Germany), and methyl orange from Sigma-Aldrich Chemie GmbH (Taufkirchen, Germany). All chemicals were used without further purification. All solutions were prepared using suprapure water. Suprapure water (declared conductivity $0.04 \mu\text{S cm}^{-1}$) was prepared by a Millipore Simplicity (USA) unit.

2.2. Procedures and Apparatus

The domains of existence of the monophasic region were already performed in the previous work and represented in a ternary phase diagram as in Figure 1.⁹

Conductivity measurements were performed at $(25 \pm 0.01)^\circ\text{C}$ using a dipping type conductivity cell Orion (model 018001) with two electrodes of bright platinum. The cell constant ($0.10402 \pm 0.00002 \text{ cm}^{-1}$) was determined by calibration with aqueous potassium chloride solutions in the concentration range from 0.001 to 0.05 mol dm^{-3} . The conductivity cell was connected to a precision component analyser Wayne-Kerr (model 6430A). Resistance (R) of test solutions was measured at four frequencies $f = 500, 800, 1000$ and 2000 Hz. Its dependence on reciprocal frequency is well presented by a straight line. Experimental procedure begins by weighing a mixtures of ethanol and citronellol (70.0 g) with various mass ratios of ethanol to citronellol ($R_{\text{E/C}}$, mass ratio of ethanol/citronellol) from 19 to 0.7 into a glass reaction cell. Carbon diox-

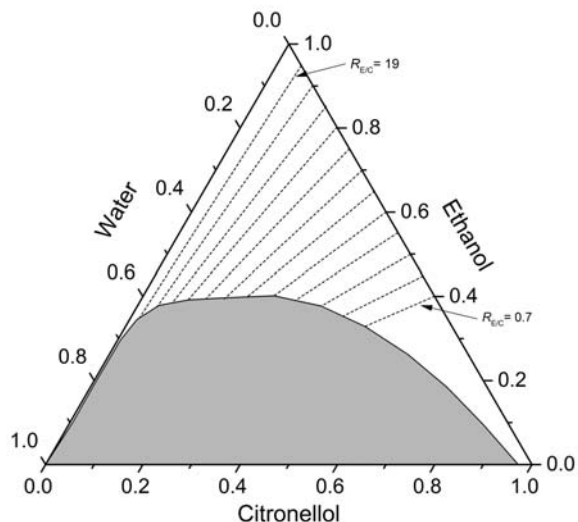


Figure 1. Ternary phase diagram of water/ethanol/citronellol mixtures at 25°C . The white region represents compositions of monophasic, clear, macroscopically homogeneous mixtures, the dark region represents compositions of two-phase systems. The values are given in mass fraction. The original diagram is taken from Ref. Š9C. The various experimental paths at different ($R_{\text{E/C}}$) values from 19 to 0.7, along which the conductivity measurements were performed, are drawn as dashed lines.

de from the atmosphere can change the electrical conductivity of mixed aqueous-organic solvents. Therefore, the reaction cell was hermetically closed with a Teflon lid after short bubbling or the solvent with high purity nitrogen. The reaction cell was then immersed into a Thermo Haake Circulator DC10-V15/B. After reaching the thermal equilibrium, the resistance at four frequencies is determined. Then the known weight of water is added into the cell using a syringe and the resistance readings are repeated. Between these two operations each test solution is homogenized through a short-run spin of a teflon magnetic stirrer bar activated by an immersible stirrer Cyclone (model 1–100 HMC).

FT-IR spectra of selected microemulsions were recorded on Shimadzu IRAffinity-1 FTIR spectrometer using CaF_2 plates, in the frequency range $4000\text{--}950 \text{ cm}^{-1}$ with 100 number scans and 4 cm^{-1} spectral resolution.

The UV-Vis spectra of selected microemulsions were performed on a computer-controlled UV-Vis spectrometer Agilent Cary 60. The path length of the quartz cell used in this experiment was 1 cm. Appropriate amounts of substances were uniformly mixed in advance and then added to the quartz cell.

3. Results and Discussion

3.1. Phase Behavior of the Water/ethanol/citronellol Ternary System

The ternary phase diagram of the water/ethanol/citronellol system at $25 \pm 0.01^\circ\text{C}$ is shown in Figure 1, in

which the component content in the system is in mass fraction. A single isotropic region extending from oil-rich to water-rich regions can be observed. The white region represents compositions of monophasic, clear, macroscopically homogeneous mixtures, and the dark region represents compositions of two-phase systems.

In general, w/o microemulsions can be formed at low water contents, in which the oil is a continuous phase. When the water content is progressively increased, the microemulsion system remains isotropic as long as there is no phase separation. As a result, there is some kind structural transition in traditional aqueous microemulsions. Similarly, for studied microemulsion system, the single-phase channels are suitable for the study of microstructure and structural transition.¹⁰

3. 2. Electrical Conductivity Measurements and Microregions of the Water/Ethanol/Citronellol Microemulsion

For surfactant-based aqueous microemulsions, Clause et al.⁷ demonstrated that, with increasing water content, the microemulsion electrical conductivity (κ) has different changes according to successive stages: (1) the initial nonlinear increase of κ reveals the existence of a percolation phenomenon that may be attributed to the inverse microdroplet aggregation; (2) the next linear increase is due to the formation of aqueous microdomains that results from the partial fusion of clustered inverse microdroplets and suggests that a w/o microemulsion is formed in the low water content region.

The variation of electrical conductivity κ with water mass fraction (ϕ_w) along dilute lines at different $R_{E/C}$ (mass ratio of ethanol/citronellol) values were determined (Figure 2).

For clarity, the plots of κ versus ϕ_w at $R_{E/C} = 4$ and 2.3 are shown in Figure 3 representing two typical examples of percolation phenomena.

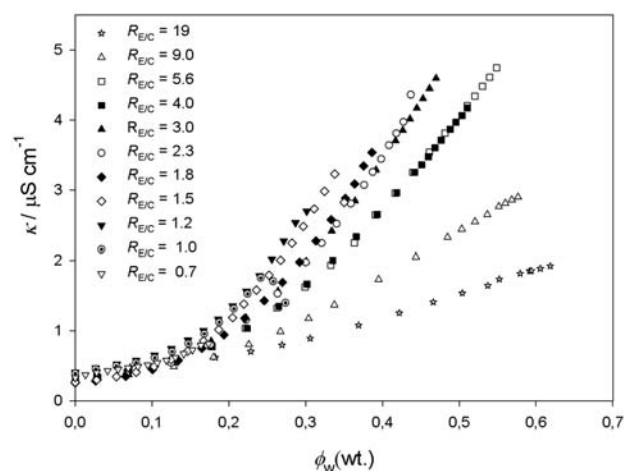


Figure 2. Conductivity κ of the microemulsion as a function of ϕ_w at different $R_{E/C}$ values.

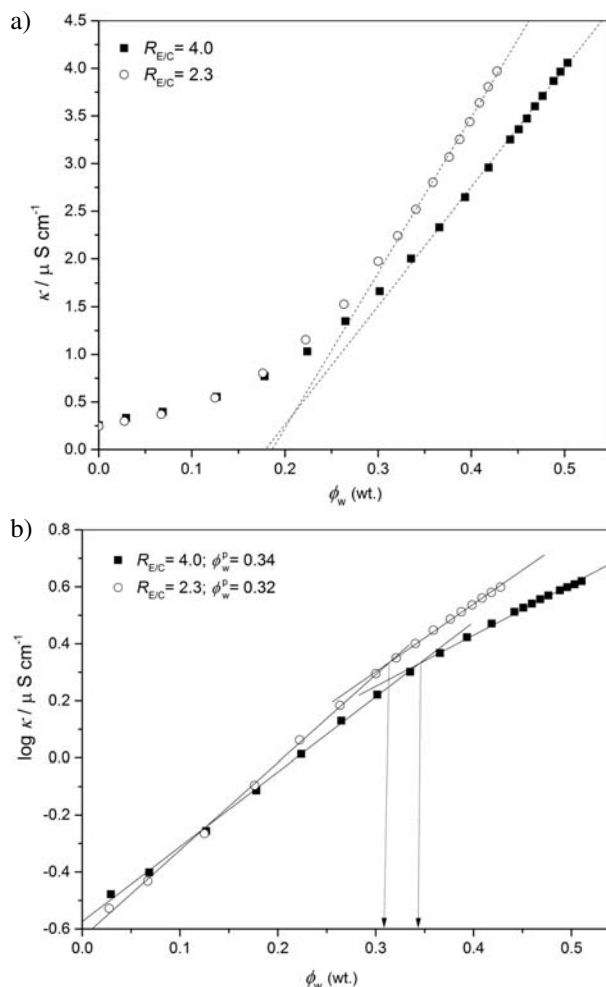


Figure 3. 3a) Electric conductivity κ of the microemulsion as a function of ϕ_w at $R_{E/C} = 4$ and 2.3. 3b) The variation of $\log \kappa$ versus weight fraction of water along the dilution line $R_{E/C} = 4$ and 2.3 (as shown in Figure 3a).

It can be seen from Figure 3a that, consistent with percolation character, electrical conductivity data increases with increment of water mass. However, due to the lack of the surfactant, conductivity enhances only within one order of magnitude. The molecule forming the interface between water droplets and the citronellol-rich surrounding medium has been found in previous studies^{2,9} unequivocally as being ethanol, and according to that in the systems studied here, the ethanol is the main component of the interfacial film whenever microstructures are present. As shown in Figure 3a, the low conductivity below ϕ_w^p suggests that the reverse droplets are discrete (isolated droplets in a non-conducting citronellol medium, forming w/o microemulsion) and show rare interaction. When the water content is raised above ϕ_w^p the value of κ increases linearly. The interaction between the aqueous domains becomes increasingly important and forms a network of conductive channel.

Figure 3b depicts the variation of $\log \kappa$ versus weight fraction of water. The change in the slope of $\log \kappa$ (Fig. 3b)

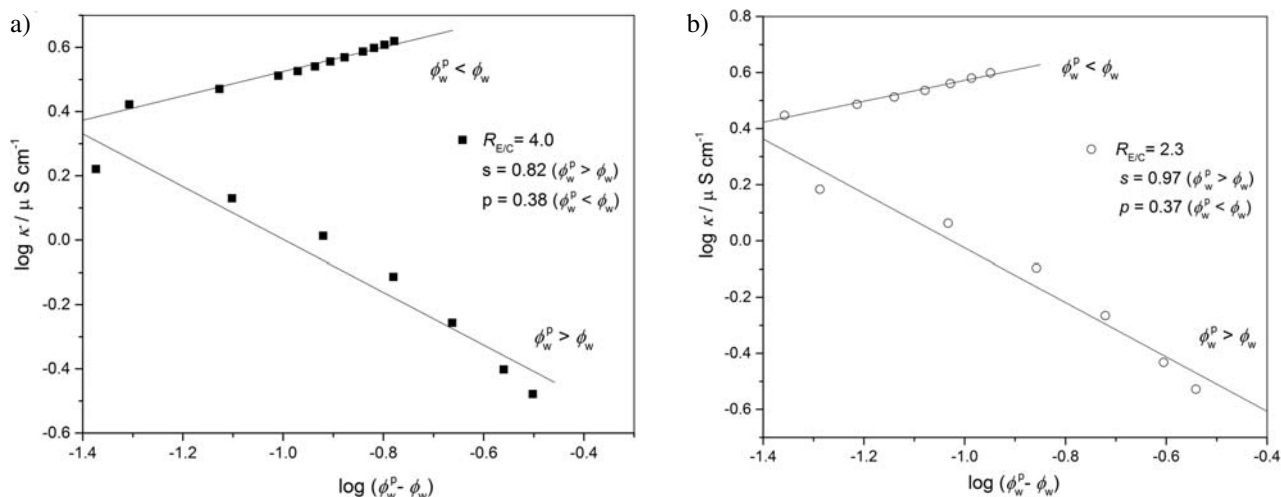


Figure 4. The scaling dependence of the conductivity, along the dilution line $R_{E/C} = 4.0$ and 2.3 , below and above the percolation threshold ϕ_w^p , on $\log(\phi_w^p - \phi_w)$. The lines are the scaling fit of the data below and above ϕ_w^p according to Eq. (1).

can be interpreted as a structural transition to bicontinuous or percolation clusters from w/o^{11} resulting with a ϕ_w^p value.

The values of s , obtained from the fitting lines in Figure 4, all fall into the prediction range of dynamic percolation theory.¹² That is to say, the barrier layer of micelles or, in this case microemulsion aggregates might be formed by short chain alcohol (in our case ethanol), although a certain amount of water molecules might permeate into it owing to the hydrogen bonding interaction between the water and short chain alcohol. Similar results on existence of microemulsion aggregates in that area are known from literature for DLS and SLS experiments.⁹ The data above the percolation threshold (Figure 4) cannot be described neither by static nor dynamic percolation theories because the values of p , obtained by fitting these data, are not in line with the theoretical value. These phenomena are possibly caused by the fact that the situation of Surfactant-Free-Microemulsions cannot satisfy the assumption of this percolation theory, namely when above ϕ_w^p , due to the hydrogen bonding interaction, more and more water molecules permeate into the barrier layer formed by the short chain alcohol (ethanol) with the increase of water weight fraction. As a consequence, the short chain alcohols cannot form an effective barrier layer of microemulsion structure, but form a solution that contains hydrogen bonded aggregates of water molecules and short chain alcohols where molecules of monoterpene (citronellol) are, depending of its weight ratio, located inside or on edges of these aggregates. These conclusions are in accordance with other studies.¹³

3. 3. UV-Vis Absorption of methyl orange (MO) in Microemulsions

The local environment within a microemulsion droplet may be characterized by UV-Vis measurements with

solvatochromic probes. MO can be used as solvatochromatic probe since its absorption spectrum is sensitive to medium effects.¹⁴ A reason for this may be that the conjugated azo group and the terminal $\text{SO}_3^- \text{Na}^+$ group of MO have different sensitivities to the micropolarity of their local environments, and play different roles in shaping the spectra. The spectral features due to the azo group seem to be more sensitive to changes in polarity. The maximum wavelength absorption band (λ_{max}) of MO shifts to shorter wavelengths upon decreasing the polarity of the medium in which the probe is located. Figure 5 shows effect of water content (ϕ_w) on the absorption spectra of methyl orange (MO) in microemulsions along the dilution line $R_{E/C} = 1.8$. The λ_{max} is situated at 464 nm in water whereas, in oil phase combined with the mass ratio of ethanol/citronellol = 1.8, it is

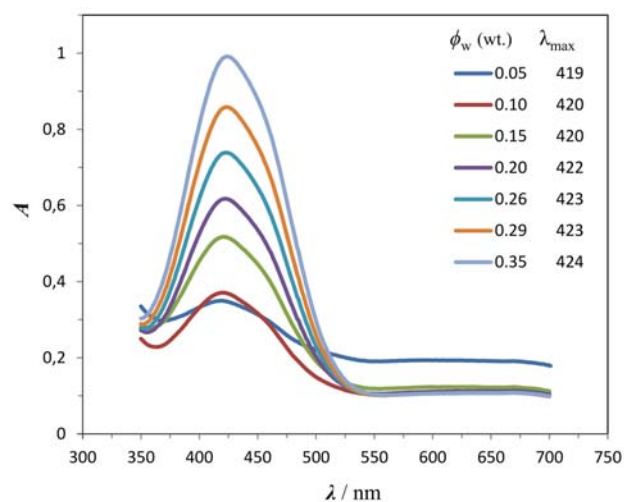


Figure 5. Effect of water content (ϕ_w) on the absorption spectra of methyl orange (MO) in microemulsions along the dilution line $R_{E/C} = 1.8$. The MO concentration is $0.110 \text{ mmol L}^{-1}$.

sitioned at 405 nm. If the position of MO in microemulsion changes, its absorption peak will also change.

As the water content in microemulsions increases (Fig. 5), the visible absorption maximum λ_{\max} of MO shifts to longer wavelengths, indicating higher polarity.^{15,16} As expected, the λ_{\max} value of methyl orange increases in the range of 419–424 nm. These results suggest that the polarity of the microenvironment of the solubilized methyl orange is intermediate between that of bulk water and ethanol, so the polarity of the water domains in the water-in-citronellol reverse microemulsion is lower than that of bulk water, which is similar to the published results.^{17,18}

3. 4. Characteristic FT-IR Spectra of Microemulsions

Available literature shows the lack of FT-IR studies regarding Surfactant-Free-Microemulsions. For the classical microemulsions FT-IR studies suggest that the reverse water interior has a multilayered structure, consisting of interfacial, intermediate, and core water.^{19,20,21}

Diferent spectra displayed in Figure 6 show the absorption bands characteristic for functional groups in molecular structure of present compounds of ternary system citronellol, ethanol, and water. The stretching referring to an OH-group is in the range 3000–3700 cm^{-1} represent the stretching of an OH-group in molecules of citronelol, ethanol, and water. The stretching relating the CH bond: CH_3 of the range 2926 to 2972 cm^{-1} and $-\text{CH}_2$ is in the range 2297 to 2350 cm^{-1} represent the stretching of citronellol and ethanol, while the stretching referring to a C = C bond is in the range of 1049–1089 cm^{-1} , and represents the stretching of citronellol. The stretching referring to an C–O-group is in the range 1350–1390 cm^{-1} , and represents the stretching of citronelol, and ethanol.

OH stretching band, previously described, is referred to the presence of ethanol, water and citronellol. The

elongation related to an OH-group is very interesting; it can be seen that by increasing the content of water in the system, it becomes wider, and finally, approaching the experimental path next to binodial curve, covers the whole area of 3000–3700 cm^{-1} . Firstly, after addition of water to studied system ($\phi_w = 0.05$) OH stretching band is located in area of low frequency 3100–3300 cm^{-1} , which is attributed to full hydrogen bonding developed between interfacial water molecules and molecules of ethanol (having the role of surfactant in our system)^{22,23}. The surface of the domains is expected to be covered with hydroxyl groups at saturation, producing a weakly associated interfacial surfactant film. After addition more water to the system and approaching the experimental path to the binodial curve, where OH stretching band becomes more and more wider covering the area of high frequency 3600–3700 cm^{-1} . That high frequency stretching is attributed to existance of free water in a “core” of micelle-like aggregation as a result of complete hydration of the hydrophilic chains. Therefore, a “core” contains a significant amount of OH groups, stemming both from ethanol and from water bound to ethanol. Finally, the sterching related to intermediate water is located between the interfacial water, and the free water from the other side to the high frequency extension.

In this surfactant-free microemulsions system, after hydration of the polar head of ethanol in an interfacial layer, stretching related to OH groups becomes broader and shifts to lower frequencies, which is well-known from classical microemulsion systems.²⁴

4. Conclusions

The dynamic percolation model classically used for surfactant-based microemulsion having a weak interfacial film, can be used to fit the conductivity data, at low water content and below the threshold of appearance of a second

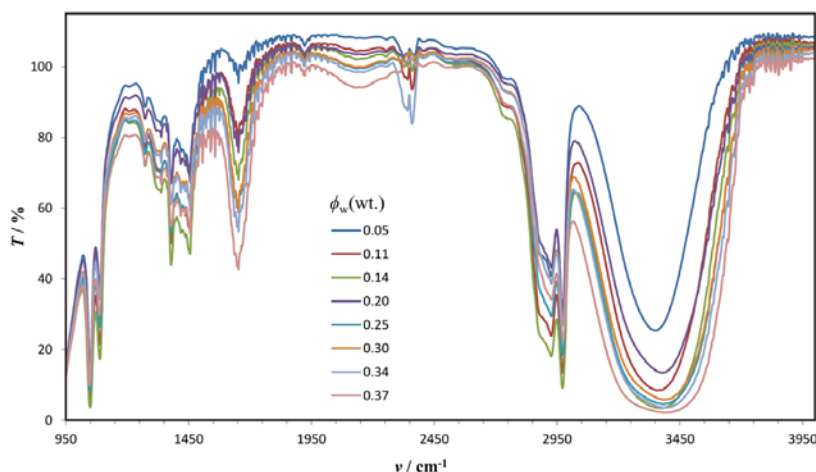


Figure 6. FT-IR spectra of microemulsions along the dilution line $R_{E/C} = 1.8$ with various water content (ϕ_w).

regime of conductivity, but this model and the static one cannot fit the conductivity data of the second regime. Like in surfactant-based microemulsions, polarity and the stretching related to an OH-group increases with increasing water content. It can be postulated from the UV-Vis wavelength absorption band (λ_{\max}) of MO and performing FT-IR spectra that the interior of the aggregates is not homogenous.

5. Acknowledgements

We would like to thank Prof. Werner Kunz for his insightful comments and encouragement, but also for the hard question which incited us to widen our research from various perspectives.

6. References

1. C. Sell (2 Ed.): The Chemistry of Fragrances – From Perfumer to Consumer, RSC Publishing, Ashford, UK, **2006**, pp. 54–91.
<http://dx.doi.org/10.1039/9781847555342>
2. P. Bošković, V. Sokol, T. Zemb, D. Touraud, W. Kunz *J. Phys. Chem. B* **2015**, *119*, 9933–9939.
<http://dx.doi.org/10.1021/acs.jpcc.5b06228>
3. S.K. Mehta, Gurpreet Kaur, K.K. Bhasin *Colloids Surf. B* **2007**, *8*, 95–104.
<http://dx.doi.org/10.1016/j.colsurfb.2007.06.012>
4. N. Peng, W.G. Hou, Chin. *J. Chem.* **2008**, *26*, 1335–1338.
<http://dx.doi.org/10.1002/cjoc.200890243>
5. S. K. Mehta, G. Kaur, K. K. Bhasin *Pharmaceut. Res.* **2008**, *25*, 227–236.
<http://dx.doi.org/10.1007/s11095-007-9355-8>
6. M. EL-Hefnawy *Mod. Appl. Sci.* **2012**, *6*, 101–105.
7. B. Lagourette, J. Peyrelasse, C. Boned, M. Clause *Nature* **1979**, *281*, 60–62.
8. O. Zech, S. Thomaier, P. Bauduin, T. Rück, D. Touraud, W. Kunz *J. Phys. Chem. B* **2009**, *113*, 465–473.
<http://dx.doi.org/10.1021/jp8061042>
9. J. Marcus, M. L. Klossek, D. Touraud, W. Kunz *Flavour Fragr. J.* **2013**, *28*, 294–299.
10. H. N. Ghosh, S. Adhikari *Langmuir* **2001**, *17*, 4129–4130.
11. F. F. Lv, L.Q. Zheng, C. H. Tung *Int. J. Pharm.* **2005**, *301*, 237–246.
<http://dx.doi.org/10.1016/j.ijpharm.2005.06.006>
12. M. Olla, M. Monduzzi *Langmuir* **2000**, *16*, 6141–6147.
13. G. D. Smith, C. E. Donelan, R. E. Barden *J. Colloid Interf. Sci.* **1977**, *60*, 488–496.
[http://dx.doi.org/10.1016/0021-9797\(77\)90313-7](http://dx.doi.org/10.1016/0021-9797(77)90313-7)
14. M. J. Clarke, K. L. Harrison, K. P. Johnston, S. M. Howdle *J. Am. Chem. Soc.* **1997**, *119*, 6399–6406.
<http://dx.doi.org/10.1021/ja9639527>
15. D. M. Zhu, Z. A. Schelly *Langmuir* **1992**, *8*, 48–50.
16. H. Gao, J. Li, B. Han, W. Chen, J. Zhang, R. Zhang, D. Yan *Phys. Chem. Chem. Phys.* **2004**, *6*, 2914–2916.
<http://dx.doi.org/10.1039/b402977a>
17. Y. A. Gao, N. Li, S. H. Zhang, L. Q. Zheng, X. W. Li, B. Dong, L. J. Yu *Phys. Chem. B* **2009**, *113*, 1389.
<http://dx.doi.org/10.1021/jp808522b>
18. X. Jie, Y. Aolin, Z. Jikuan, L. Dongxiang, W. G. Hou *J. Phys. Chem. B* **2013**, *117*, 450–456.
<http://dx.doi.org/10.1021/jp310282a>
19. T. Tamura, Z. A. Schelly *J. Am. Chem. Soc.* **1981**, *103*, 1013–1018.
<http://dx.doi.org/10.1021/ja00395a003>
20. A. Goto, H. Yoshita, H. Kishimoto, T. Fujita *Langmuir* **1992**, *8*, 441–445.
21. G. Onori, A. Santucci *J. Phys. Chem.* **1993**, *97*, 5430–5434.
<http://dx.doi.org/10.1021/j100122a040>
22. N. Akter, S. Radiman, F. Mohamed, I. A. Rahman, M. I. H. Reza *Sci. Rep.* **2011**, *71*, 1–5.
23. C. Gonzalez-Blanco, L. J. Rodriguez, M. M. Velazquez *Langmuir* **1997**, *13*, 1938–1945.
24. W. Fang, B. Fang, Z. Zhang, S. Zhang *J. Dispersion Sci. Technol.* **2008**, *29*, 1166–1172.
<http://dx.doi.org/10.1080/01932690701686858>

Povzetek

Nedavno je bil ugotovljen obstoj nanostruktur v trokomponentnem sistemu voda-etanol-citronelol, kar smo v tem delu proučevali z meritvami električne prevodnosti ter z UV-Vis in FT-IR spektroskopskima metodama. Iz meritev prevodnosti je možno sklepati na povečanje polarnosti polarne psevdofaze z dodatkom vode in – podobno kot v klasičnih mikroemulzijah, temelječih na surfaktanih – celo na prisotnost prostih molekul v primeru večje množine prisotne vode v sistemu. Tudi tu smo za razlago poteka prevodnosti pod kritično vsebnostjo vode (ϕ_w^p) lahko uporabili dinamični perkolacijski model, ki dobro opisuje obnašanje klasičnih mikroemulzij, ki tvorijo šibek film med dvema fazama. V pristnosti večje množine vode, nad ϕ_w^p , dobljenih vrednosti prevodnosti ni mogoče več razložiti niti s statičnim niti z dinamičnim perkolacijskim modelom. Enako kot pri klasičnih mikroemulzijah, je tudi pri proučevanem sistemu povečanje polarnosti mikrookolja z naraščajočo vsebnostjo vode možno dokazati z UV-Vis spektroskopijo s pozicijo maksimalne absorpcije (λ_{\max}) barvila metil oranž ter FT-IR spektroskopijo.